Acta Cryst. (1994). D**50**, 258-262

Solid-State Phase Transition in the Crystal Structure of Ribulose 1,5-Bisphosphate Carboxylase/Oxygenase

BY KAM Y. J. ZHANG AND DAVID EISENBERG

Molecular Biology Institute and Department of Chemistry and Biochemistry, University of California, Los Angeles, CA 90024-1570, *USA*

(*Received* 19 *May* 1993; *accepted* 22 *November* 1993)

Abstract

The crystal structure is described of ribulose 1,5-bisphosphate carboxylase/oxygenase in a new crystal form. This new form (form V) was obtained from a previously known crystal form (form III) through a solid-state phase transition. The solid-state phase transition was brought about by transferring the crystal from a high-salt low-pH mother liquor to a low-salt high-pH synthetic mother liquor. The interplay of electrostatic repulsion and osmotic pressure induced a unit-cell shrinkage of 24 Å along the *c* axis and expansion of 4 Å along the *a* and *b* axes. The space group also changed from *I*422 to *I*4. The new crystal form was shown to be more resistant to X-ray radiation damage, which suggests the effect of crystal stabilization by non-penetrating molecules. The structure of ribulose 1,5-bisphosphate carboxylase/oxygenase in the new crystal form is compared with that of the old crystal form.

1. Introduction

Solid-state phase transition is a phenomenon which has been widely studied in metals, alloys and other solids (Wayman, 1971). The physical properties of solids can change dramatically upon phase transition. New materials with altered physical and mechanical properties can often be obtained by inducing a solid-state phase transition. There are also many documented cases of solid-state phase transition in the crystals of small molecules (Salje, 1991). However, solid-state phase transitions in the crystals of macromolecules are rarely reported. The solid-state phase transition of insulin crystals was studied by Reynolds *et al.* (1988) using a synchrotron-radiation Laue-diffraction method. Also, Hajdu *et al.* (1987) reported a transient phenomenon in crystals of glycogen phosphorylase *b*.

Ribulose 1,5-bisphosphate carboxylase/oxygenase (RuBisCO, E.C. 4.1.1.39) is a bifunctional enzyme that catalyzes the carboxylation and oxygenation of ribulose 1,5-bisphosphate (RuBP) in the initial steps of photosynthetic carbon fixation and photorespiration. The incorporation of atmospheric carbon into the biosphere is accomplished almost entirely through the carboxylation of RuBP with CO_2, catalyzed by RuBisCO (Brändén, Lindqvist & Schneider, 1991). RuBisCO, being the most abundant enzyme on earth, yet at the same time a grossly inefficient enzyme, has attracted systematic efforts to understand its catalytic mechanism. The goal is genetic redesign, aimed at improving its catalytic efficiency (Ellis, 1979; Andrews & Lorimer, 1987). To facilitate this goal, crystal structures of RuBisCO from various sources have been solved by X-ray crystallography (Schneider, Lindqvist, Brändén & Lorimer, 1986; Chapman, Suh, Cascio, Smith & Eisenberg, 1987; Chapman *et al.*, 1988; Andersson *et al.*, 1989; see Brändén *et al.*, 1991, for a review).

We describe here a new form of RuBisCO crystal which was obtained from a form previously known through a solid-state phase transition. The structure and diffraction properties of RuBisCO in the new form are compared with that of the old form.

2. Experimental

2.1. *Purification and crystallization*

RuBisCO was purified from the leaves of the Turkish samsun variety of *Nicotiana tabaccum* as described by Chan, Sing & Wildman (1972) and Chapman *et al.* (1986). RuBisCO was stored in 50 m*M* KH_2PO_4, 0.5 m*M* EDTA and 0.5 m*M* NaN_3 at pH 7.2 with the protein concentration about 28 mg ml^{-1}. Crystals (form III) were grown according to a modified procedure of Baker, Suh & Eisenberg (1977) using the hanging-drop method. The reservoir contained the precipitant, which is made of 0.2 *M* KH_2PO_4, 0.3 *M* $(NH_4)_2SO_4$ and 1 m*M* NaN_3 at pH 5.2. The hanging drop consisted of RuBisCO solution and precipitant mixture between 30 and 70%(*v*/*v*). Large crystals of bipyramidal shape were grown within 1-2 weeks.

2.2. *Crystal transformation*

RuBisCO is catalytically active only when it forms a ternary complex of RuBisCO-CO_2Me^{2+} (Lorimer, Badger & Andrews, 1976; Lorimer, 1981). This is achieved at alkaline pH with CO_2 and divalent metal ions. Because our earlier work (Chapman *et al.*, 1987; Curmi, Cascio, Sweet, Eisenberg & Schreuder, 1992) with form III crystals was at low pH with unactivated enzyme,

ISSN 0907-4449

we were interested in learning the structural differences between RuBisCO at acidic and alkaline pH. For this reason, a form III crystal was transferred from its mother liquor of high salt at pH 5.2 to a low-salt synthetic mother liquor which consists of 20%(*w*/*v*) polyethylene glycol 8000 (PEG 8000), 50 m*M* MES [2-(*N*-morpholino)ethanesulfonic acid], 50 m*M* NaCl and 1 m*M* NaN_3 at pH 5.2. After a quick wash, the crystal was subsequently transferred into a low-salt high-pH and high PEG 8000 concentration activation buffer. This activation solution is made of 42%(*w*/*v*) PEG 8000, 50 m*M* TRIS [tris(hydroxymethyl)aminomethane], 50 m*M* NaCl, 10 m*M* $MgCl_2$, 20 m*M* $NaHCO_3$ and 1 m*M* NaN_3 at pH 8.0. The crystal underwent a solid-state phase transition upon transfer. Gradual transfer of crystals was tested in multiple increments of pH and PEG 8000 concentrations. A smooth increase of pH and PEG 8000 concentration, obtained by using dialysis membranes, was also tried. Both these gradual transfer techniques destroy the diffraction power of the crystals. Only the direct transfer of crystals from high-salt low-pH mother liquor to high-pH low-salt synthetic mother liquor produced diffraction-quality crystals. Various concentrations of the PEG 8000 were tested in order to find the optimum condition for the crystal transfer. At lower PEG 8000 concentrations the crystal displays many tiny cracks (expansion cracks) upon the increase of pH, whereas at higher PEG 8000 concentrations, the crystal shows a few large cracks (contraction cracks) upon the increase of pH from 5.0 to 8.0. Even at the optimum PEG 8000 concentrations, we still observe a few cracks in the crystal upon transfer. However, these cracks gradually disappear after a few days, showing an annealing process in the crystal. By recording the X-ray diffraction pattern of the crystal at time intervals after transfer, we observed an order-disorder-reorder process. The crystal lost its diffraction power soon after the transfer. When tested by X-rays about 3 days after transfer, the crystal diffracts only to about 8 Å resolution. However, the crystal regains its diffraction power to 2.5 Å about 10 days after transfer, suggesting that the solid-state phase transition took about 10 days for completion.

2.3. *Form* V *properties and data collection*

The space group of the new crystal form (form V) is *I*4 which was determined by precession photographs of all principal zones. Full data were collected from a single crystal using a Xuong-Hamlin multiwire area detector (Hamlin, 1985) with Cu $K\alpha$ radiation from a Rigaku rotating-anode generator. Form V crystals diffract to the same resolution as form III crystals, but are much more resistant to X-ray radiation damage. This enables full data to be collected from a single form V crystal. Data collection and processing were carried out by a software package written by Larry Weissman (1979). The data consist of 38 575 unique reflections (which comprise 84% of all possible reflections to 2.5 Å resolution) with an R_{merge} value of 8.3% on intensities. Table 1 compares the space group, unit-cell dimensions and the Matthews' coefficient (Matthews, 1974) for the two crystal forms. Notice the enormous differences in unit-cell dimensions.

Table 1. *Comparison of space groups and cell dimensions for RuBisCO form* III *and* V *crystals*

	Space group	a (Å)	c (Å)	V_m (Å^3 Da^{-1})	Asymmetric unit
Form III	*I*422	148.7	137.5	3.16	L_1S_1*
Form V	*I*4	153.0	113.5	2.74	L_2S_2

* Here L and S represent the large and small subunits of RuBisCO, respectively.

3. Structure solution and description

The structure of RuBisCO form V was determined by molecular replacement, using the atomic structure of the heterodimer (*LS*; *L* - large subunit, *S* - small subunit) in form III (Curmi *et al.*, 1992) as a search model. The molecular replacement and structure refinement were carried out using *X-PLOR* (Brünger, 1990). The self-rotation function of the form V data showed the orientation of the non-crystallographic twofold axis at spherical polar angles of (45, 0, 180°) with peak height of 6σ [σ is the root-mean-square (r.m.s.) deviation of the rotation function]. The next highest peak was at 2σ. This non-crystallographic twofold axis corresponds to the crystallographic twofold axis in form III crystals along the *ab* diagonal. The initial cross-rotation function revealed the orientation of the two RuBisCO molecules in the asymmetric unit. The solutions of the cross rotation search were at spherical polar angles of (0, 0, 0°) and (45, 0, 180°) with peak heights of 9 and 8σ, respectively. The next highest peak was at 4σ. The rotation- function solution was subsequently refined by the Patterson correlation (PC) method in *X-PLOR*. The orientations of the two molecules in the asymmetric unit were refined to spherical polar angles of (93.96, 91.90, 3.78°) and (46.96, 179.88, 180.15°), respectively.

The positions of the two non-crystallographic symmetry-related molecules in the asymmetric unit and their relative displacement were found by the translation function. The search model of RuBisCO heterodimer (*LS*) from form III was rotated according to the first PC-refined orientation (93.96, 91.90, 3.78°) and a translation search was subsequently carried out along the *ab* plane, since the position of the first molecule along the *c* axis is arbitrary in space group *I*4. This gave a solution of (0.052, 0.987, 0) in fractional coordinates with peak height of 8σ. The search model was also rotated according to the second PC-refined orientation (46.96, 179.88, 180.15°) and then a translation search was performed along the *ab* plane. This yielded a

solution of (0.487, 0.447, 0) in fractional coordinates with peak height of 8σ. The search models were translated to their respective positions on the *ab* plane. The relative disposition between the first and the second molecule in the asymmetric unit was determined by a translation search along the *c* axis. This gave a solution of (0, 0, 0.304) in fractional coordinates with peak height of 7σ. After positioning the form III RuBisCO model in the form V cell, a rigid-body refinement was carried out. The large and small subunits were allowed to move with respect to each other as rigid bodies. This improved the initial *R* factor from 0.34 to 0.31.

Further positional refinement and simulated-annealing refinement were performed using *X-PLOR*. The model was readjusted according to the $2F_o - F_c$ maps using *FRODO* (Jones, 1985) and refinement was repeated. The final structure has an *R* factor of 21.1% for all the data from 8.0 to 2.5 Å with r.m.s. deviations from ideal for bond lengths of 0.018 Å and bond angles of 3.83°. The dihedral angles as examined in the Ramachandran plot (Ramachandran & Sasisekharan, 1968) are all in allowed regions.

The unit-cell transformation and the molecular packing of forms III and V are compared in Fig. 1. It can be seen that the form III unit cell (dashed line) shrinks by 24 Å along the *c* axis and expands about 4 Å along the *a* and *b* axes to yield the new form V unit cell (solid line). The result is a shrinkage of 14% in volume. The Matthews' coefficient, V_m, changes from 3.16 to 2.74 $Å^3\ Da^{-1}$ (Matthews, 1974). This remarkable cell transformation is achieved by the rotation of the first RuBisCO heterodimer (*LS*) in the asymmetric unit by 3.78° around spherical polar axis (93.96, 91.90°), the rotation of the second RuBisCO heterodimer (*LS*) in the asymmetric unit by 0.15° around spherical polar axis (46.96, 179.88°), and a 24 Å translation of the two non-crystallographically related RuBisCO molecules (L_2S_2) with respect to their body-center-related counterparts, from a form III to a form V cell. There are 60 more intermolecular contacts in form V than in form III for the RuBisCO heterodimer of large and small subunits. The solvent-accessible areas of the *LS* heterodimer in form III and form V are 29 218 and 28 945 $Å^2$, respectively.

The structures of RuBisCO at acidic (form III) and alkaline pH (form V) are very similar except in the N-terminal region (residues 90-95), the loop 6 region (residues 332-338) and the C-terminal α-helix (residues 460-467), as shown in Fig. 2.

Comparison of the enzyme active sites in forms III and V RuBisCO are shown in Fig. 3. The most noticeable difference is that the three phosphate groups which bind in the active site of form III RuBisCO (Curmi *et al.*, 1992) are absent in form V RuBisCO. No significant changes were observed in the active-site residues of these two structures. No significant peaks were found in the $F_o - F_c$ difference map at the putative site for carbamate and magnesium. Because activated RuBisCO is carbamylated at Lys201 and bound to an Mg^{2+} ion, it appears that RuBisCO has not been activated in the form V crystal under the activation conditions containing 42% PEG 8000. This absence of activation may be related to the presence of a high concentration of PEG 8000 at 42%(*w*/*v*). Since the phosphate ions have relatively low binding affinity to RuBisCO (Siegel, Wishnick & Lane, 1972) and can be easily removed from the crystal by a desalting procedure (Zhang, Cascio &

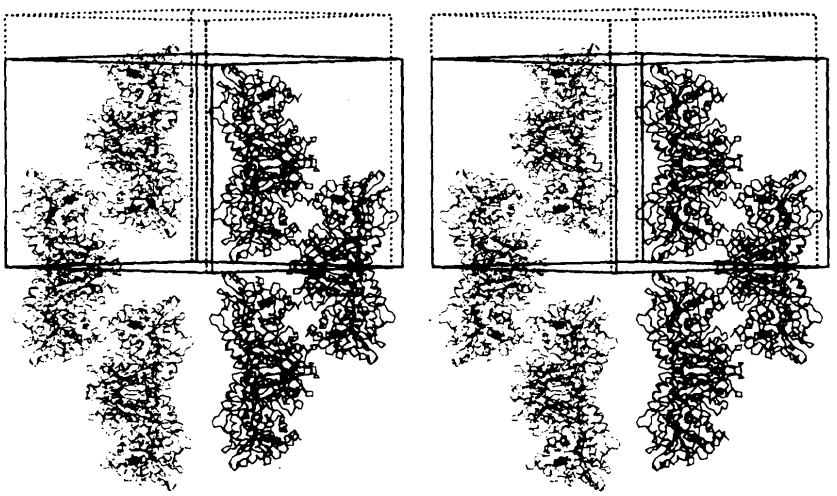

Fig. 1. Unit-cell dimensions and intermolecular interactions in RuBisCO crystal forms III and V, shown as a stereo pair. The form III cell and chains are shown in dashed lines, whereas the form V cell and chains are represented by solid lines. Three Cα dimer models of RuBisCO are shown for each form, each dimer consisting of two large and two small subunits (L_2S_2). The middle dimer in the form III cell can be superposed onto the form V dimer by crystallographic twofold rotation about the *c* axis. For clarity, the equivalent dimers are shown for form III and form V, and only contacting dimers. The actual unit cell contains $(LS)_{16}$.

Eisenberg, 1994), the phosphate ions are likely to be removed from RuBisCO during the crystal transfer from the high-salt (containing phosphate and sulfate) mother liquor at pH 5.2 to the low-salt (free of phosphate and sulfate) activation buffer at pH 8.0 and with 42%(*w*/*v*) PEG 8000.

4. Discussion and summary

The solid-state phase transition observed in the RuBisCO crystals is the result of the interplay of two counteracting forces exerted on the crystal, electrostatic and osmotic. The change of pH from 5.2 to 8.0 shifted the pH above the p*I* (5.0) by 3.0 pH units. Since there are 15 histidine residues per RuBisCO molecule (*LS*), the net charge is increased by 120 electrons per L_8S_8 molecule. This increases the electrostatic repulsions of charged residues. It seems likely that this electrostatic repulsion forces molecules away from each other and causes expansion cracks. However, PEG 8000 creates a substantial osmotic pressure on the crystal, because its large size prevents penetration into the crystal. This osmotic pressure causes contraction cracks observed as a few large cracks in the crystal. These two forces balance out at some combinations of pH and PEG concentration. The pH and PEG concentration values of our experiment appear to be satisfactory and somehow prevent the molecules in the crystal from becoming misaligned during expansion

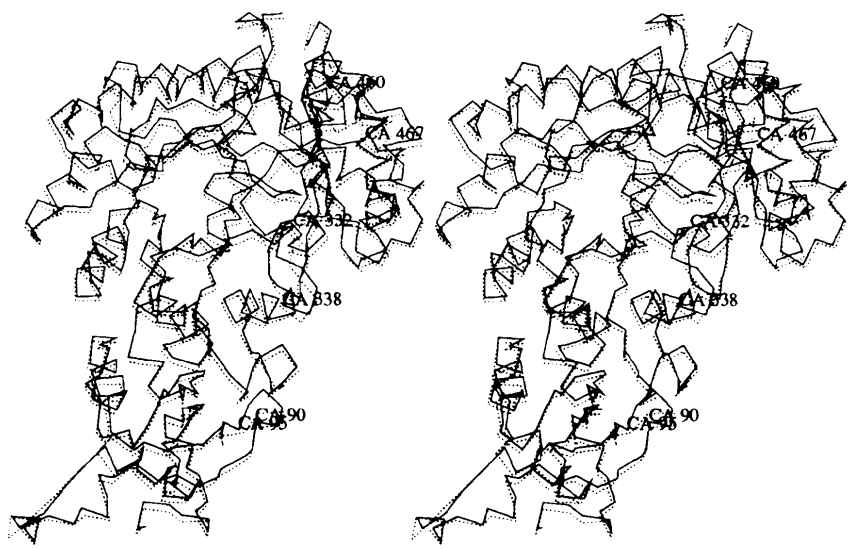

Fig. 2. Superposition of the Cα atoms of RuBisCO large and small subunits in form III and V crystals. RuBisCO molecules in form III and V are shown in dashed and solid lines, respectively. The regions with the greatest differences are marked by labels: these are residues 90-96 near the N terminus, residues 332-339 in the loop 6 region and residues 460-467 at the C terminus. The small subunit is at the upper left.

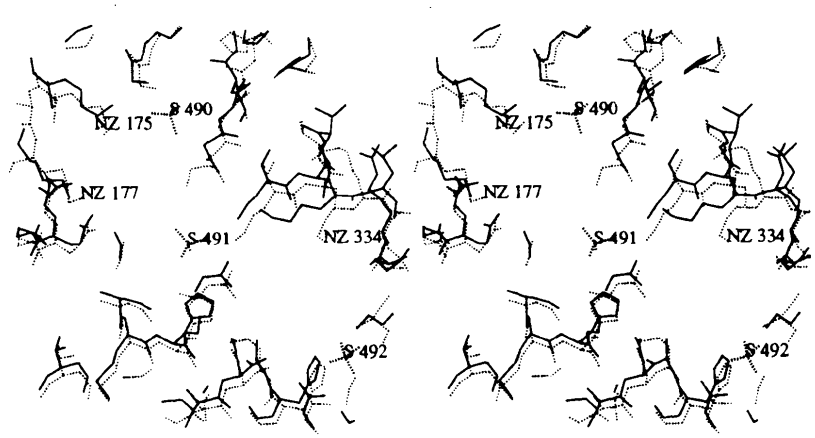

Fig. 3. The active-site region shown as a stereo pair. Residues in forms III and V are shown as dashed and solid lines, respectively. The three phosphate groups in the form III RuBisCO are indicated by labels S490, S491 and S492, which are highlighted with thick dashed lines.

cracking. The osmotic pressure exerted by PEG 8000 on the crystal provides an opportunity for annealing and this induces a massive change of the unit cell. The result is that some 14% of solvent is squeezed from the crystal.

During the solid-state phase transition, RuBisCO molecules shift about 24 Å along the *c* axis. The result is that the center-to-center distance along the *c* axis between two stacked hexadecamers equals the height of a single hexadecamer along the *c* axis. The intermolecular contacts are increased. There is more buried surface area after the phase transition. The packing is also much tighter after the phase transition, with the Matthews' coefficient decreased from 3.16 to 2.74 $Å^3 Da^{-1}$. The form V crystal is more resistant to X-ray damage because of the tighter packing and more extensive intermolecular interactions. The effect of crystal stabilization by PEG was observed by Cascio, Williams & McPherson (1984). Ray *et al.* (1991) also examined the stabilization effect of PEG on the crystals of phosphoglucomutase, and also found improved crystal quality. These examples suggest that it is feasible to stabilize the crystal by non-penetrating high-molecular-weight molecules and to obtain better quality crystals.

The structural details of the RuBisCO molecule remain largely unchanged upon this phase transition and change in pH. The r.m.s. difference between the RuBisCO structure in form III and form V crystals is 1.20 Å for all atoms and 0.89 Å for main-chain atoms.

We thank Dr Duilio Cascio and Jeanne Perry for their help in RuBisCO crystallization, Dr Matthias Wilmanns for discussion, and NIH for support. The structure refinement was performed on the Cray Y-MP of the San Diego Supercomputer Center. The coordinates have been deposited with the Protein Data Bank.*

* Atomic coordinates and structure factors have been deposited with the Protein Data Bank, Brookhaven National Laboratory (Reference: 1RLD, R1RLDSF). Free copies may be obtained through The Technical Editor, International Union of Crystallography, 5 Abbey Square, Chester CH1 2HU, England (Supplementary Publication No. SUP 37107). A list of deposited data is given at the end of this issue.

References

ANDERSSON, I., KNIGHT, S., SCHNEIDER, G., LINDQVIST, Y., LUNDQVIST, T., BRÄNDÉN, C.-I. & LORIMER, G. H. (1989). *Nature (London)*, **337**, 229-234.

ANDREWS, T. J. & LORIMER, G. H. (1987). *The Biochemistry of Plants*, Vol. 10, edited by M. D. HATCH & N. K. BOARDMAN, pp. 131-218. Orlando: Academic Press.

BAKER, T. S., SUH, S. W. & EISENBERG, D. (1977). *Proc. Natl Acad. Sci. USA*, **74**, 1037-1041.

BRÄNDÉN, C.-I., LINDQVIST, Y. & SCHNEIDER, G. (1991). *Acta Cryst.* B**47**, 824-835.

BRÜNGER, A. T. (1990). *X-PLOR.* Version 2.1. *A System for Crystallography and NMR.* Yale Univ., New Haven, Connecticut, USA.

CASCIO, D., WILLIAMS, R. & MCPHERSON, A. (1984). *J. Appl. Cryst.* **17**, 209-210.

CHAN, P. H., SING, K. S. S. & WILDMAN, S. G. (1972). *Science*, **176**, 1145-1146.

CHAPMAN, M. S., SMITH, W. W., SUH, S. W., CASCIO, D., HOWARD, A., HAMLIN, R., XUONG, N.-H. & EISENBERG, D. (1986). *Philos. Trans. R. Soc. London Ser. B*, **313**, 367-378.

CHAPMAN, M. S., SUH, S. W., CASCIO, D., SMITH, W. W. & EISENBERG, D. (1987). *Nature (London)*, **329**, 354-356.

CHAPMAN, M. S., SUH, S. W., CURMI, P. M. G., CASCIO, D., SMITH, W. W. & EISENBERG, D. (1988). *Science*, **244**, 71-74.

CURMI, P. M. G., CASCIO, D., SWEET, R. M., EISENBERG, D. & SCHREUDER, H. (1992). *J. Biol. Chem.* **267**, 16980-16989.

ELLIS, R. J. (1979). *Trends Biochem. Sci.* **4**, 241-244.

HAJDU, J., MACHIN, P. A., CAMPBELL, J. W., GREENHOUGH, T. J., CLIFTON, I. J., ZUREK, S., GOVER, S., JOHNSON, L. N. & ELDER, M. (1987). *Nature (London)*, **329**, 178-181.

HAMLIN, R. (1985). *Methods Enzymol.* **114**, 416-452.

JONES, T. A. (1985) *Methods Enzymol.* **115**, 157-171.

LORIMER, G. (1981). *Biochemistry*, **20**, 1236-1240.

LORIMER, G., BADGER, M. R. & ANDREWS, T. J. (1976). *Biochemistry*, **15**, 529-536.

MATTHEWS, B. W. (1974). *J. Mol. Biol.* **82**, 513-526.

RAMACHANDRAN, G. N. & SASISEKHARAN, V. (1968). *Adv. Protein Chem.* **23**, 325-342.

RAY, W. J. JR, BOLIN, J. T., PUVATHINGAL, J. M., MINOR, W., LIU, Y. & MUCHMORE, S. W. (1991). *Biochemistry*, **30**, 6866-6875.

REYNOLDS, C. D., STOWELL, B., JOSHI, K. K., HARDING, M. M., MAGINN, S. J. & DODSON, G. G. (1988). *Acta Cryst.* B**44**, 512-515.

SALJE, E. K. H. (1991). *Acta Cryst.* A**47**, 453-469.

SCHNEIDER, G., LINDQVIST, Y., BRÄNDÉN, C.-I. & LORIMER, G. (1986). *EMBO J.* **5**, 3409-3415.

SIEGEL, M. I., WISHNICK, M. & LANE, M. D. (1972). *Enzymes*, **6**, 169-192.

WAYMAN, C. M. (1971). *Annu. Rev. Mater. Sci.* **1**, 185-218.

WEISSMAN, L. (1979). PhD dissertation, Univ. of California, Los Angeles, USA.

ZHANG, K. Y. J., CASCIO, D. & EISENBERG, D. (1994). *Protein Sci.* **3**, 64-69.